



# Audio Engineering Society Convention Paper

Presented at the 127th Convention  
2009 October 9–12 New York NY, USA

*The papers at this Convention have been selected on the basis of a submitted abstract and extended precis that have been peer reviewed by at least two qualified anonymous reviewers. This convention paper has been reproduced from the author's advance manuscript, without editing, corrections, or consideration by the Review Board. The AES takes no responsibility for the contents. Additional papers may be obtained by sending request and remittance to Audio Engineering Society, 60 East 42<sup>nd</sup> Street, New York, New York 10165-2520, USA; also see [www.aes.org](http://www.aes.org). All rights reserved. Reproduction of this paper, or any portion thereof, is not permitted without direct permission from the Journal of the Audio Engineering Society.*

---

## Optimising the re-enforcement effect of early reflections on aspects of live musical performance using the image source method

Michael Terrell<sup>1</sup>, and Joshua D. Reiss<sup>1</sup>

<sup>1</sup>Queen Mary, University of London, Center for Digital Music, UK

Correspondence should be addressed to Michael Terrell ([Michael.Terrell@elec.qmul.ac.uk](mailto:Michael.Terrell@elec.qmul.ac.uk))

### ABSTRACT

The image source method is used to identify early reflections which have a re-enforcement effect on the sound traveling within an enclosure. The distribution of absorptive material within the enclosure is optimised to produce the desired re-enforcement effect. This is applied to a monitor mix and a feedback prevention case study. In the former it is shown that the acoustic path gain of the vocals can be increased relative to the acoustic path gain of the other instruments. In the latter it is shown that the acoustic path from loudspeaker to microphone can be manipulated to increase the perceived signal level before the onset of acoustic feedback.

### 1. INTRODUCTION

The acoustics of a performance space have a significant effect on the mix that a listener experiences. Room acoustic models seek to describe sound transfer from source to listener within an enclosure. The sound heard is a combination of the direct sound from the source and all reflections from the boundaries of the enclosure. A dead room has absorbent walls so the reflections are weak when compared to the direct sound. A lively room has reflective walls

so the reflections are strong when compared to the direct sound. In general people feel uncomfortable in a room which is too dead, primarily because this is a very unnatural environment, to which exposure in every day life is limited. Very lively rooms can sound messy and can reduce intelligibility, particularly of spoken word. Moderately reverberant rooms are generally preferred.

There is a significant body of work in the literature on room acoustics. Kuttruff's Room Acoustics [1], is a standard text on the subject. The effect of an

enclosure on the sound at a given location is caused by reflections of the sound source. These are broadly classified as either early reflections or the reverberant tail, with an area of transition in between. The early reflections are discrete instances of the sound source hitting a given boundary (or combination of boundaries) and reaching the listener. The reverberant tail contains a diffuse, distribution of many late reflections. The main measurement of a room's acoustic properties is the time over which an initial impulse will decay by 60 dB ( $RT_{60}$ ). This is known as the reverberation time. The type of analysis used depends on the size of the space. An empirical equation to calculate the reverberation time of a large room was first defined by W. C. Sabine in the late 1800s. In such a room, the models used assume that there is a sufficient density of reflections, and the reflections are sufficiently diffuse that an averaging effect occurs, and a statistical measure of the reverberation is appropriate. In small spaces there are insufficient reflections to justify the statistical approach, hence a deterministic approach is used.

Geometrical room acoustic models simplify the description of a sound wave to that of a ray. The wave is divided into discrete quanta of sound energy. No information regarding the wavelength or phase of the signal is included. This has two main implications. If the wavelength of a sound wave is sufficiently large, its behaviour will be affected by the dimensions of the enclosure in which it travels. Geometrical methods are therefore not able to model behaviour such as standing waves or diffraction. Thus, it is therefore only valid to apply geometrical methods to high frequency signals. The frequency below which the method is no longer valid is dependent on the size of the enclosure. It is suggested in [1] that the dimensions of the enclosure should be an order of magnitude greater than the wavelength. Secondly, interference between waves cannot be modeled as the rays do not have phase. This assumption holds up well in most situations as it can be assumed that sound signals within an enclosure are incoherent.

The two prominent geometrical methods are the ray tracing method and the image source method. Both methods use the assumptions detailed above but differ in how the rays are tracked. The ray tracing method was first proposed by Krokstad [2]. Sound waves emanating from a source are discretised into

individual rays. Each ray is tracked over a given time period. Reflections were initially modeled as being specular, i.e. the angle of reflection is equal to the angle of incidence, and the energy of the reflected sound is also contained within a ray (there is no dispersion). A frequency independent absorption coefficient was applied to reduce the energy contained in the ray. The sound reaching a given location is found by integrating the rays over space and time. The image source model is presented by Gibbs et al. [3] and an example implementation is demonstrated by Allen et al. [4]. The image source model does not track the rays. Instead, the static, virtual position of reflected sources are identified by plotting images of the room and source. Each path from an image source to the receiver represents a reflected path with specular reflections. Absorption is applied in the same way as the ray tracing model.

There have been advancements in the reflection models used in geometrical methods in order to incorporate diffuse reflections. Diffuse reflections result in a more even distribution of energy within the sound field. An entirely diffuse reflection is characterised by a reflected energy distribution which is independent of the angle of incidence [1]. The distribution of energy will take place according to Lambert's cosine law. In reality a reflection will have components which are both specular and diffuse. The ray tracing method has been developed to accommodate diffuse reflections. A probability is assigned to the likelihood that a particular reflection will be specular or diffuse. This is based on the surface material of the boundary in question. If the reflection is diffuse it is modeled by randomising the direction of the reflected ray, subject to the probability distribution given by Lambert's cosine law. The necessity for a diffusion model to accurately predict room response was demonstrated by Hodgson [5]. Hodgson compared the room response prediction obtained using the image source model with the experimental room response. The discrepancies between the two were consistent and indicated the presence of diffuse reflections. This was confirmed using a ray tracing model which accounted for diffuse surface reflections. Dalenback [6] presented a unified approach which incorporated both diffuse and specular reflections. The method used cone tracing to handle the diffuse reflections. An initial analysis identifies where spec-

ular reflections occur. At each point identified the energy of the specular reflection is stored. A second analysis is performed with each area of stored energy acting as a diffuse source. Embrechts [7] highlighted the computational expense of the random diffusion model, particularly when the probability function used was frequency dependent. Frequency dependency is required for an accurate model, but results in multiple processing for each frequency band. Embrechts demonstrated a method which enabled all frequency components to be considered in a single pass, greatly reducing the processing time. Diffusion effects were included in the image source model by Dalenback et al. [8] by introducing scattering at points of reflection. Elements of the standard ray tracing method were introduced to model the late part of the room response. The result was an improvement in efficiency, whilst retaining the highly detailed early part of the room response. A further extension to the image source model was presented by Borish [9] to allow it to be applied to arbitrarily shaped polyhedra.

An alternative to geometrical methods are the finite element methods, of which the digital waveguide mesh is the most prominent. A review of the digital waveguide mesh method was presented by Murphy et al. [10]. In a waveguide model, the space (whether 2D or 3D) to be modeled is discretised into a uniformly spaced sampling grid (the mesh). Each node in the grid is a scattering junction. If a pressure disturbance is introduced into the mesh at a given junction, it is scattered to neighbouring junctions. The pressure transferred is a function of the impedance in the transfer path. The propagation of the sound wave is captured by sampling at regular time intervals, and calculating the propagation between all adjacent junctions in each interval. There is a limit to the maximum frequency at which the waveguide mesh can be used, based on the spatial resolution of the mesh. The first application of the method to simulation of room acoustics was presented by Savioja et al. [11]. The benefit of waveguide mesh models is that they implicitly include effects such as diffraction and refraction. Boundary node models have been presented which capture different types of boundary behavior. Lee et al. [12] demonstrate diffusing boundary implementations in a 2-D digital waveguide mesh. Murphy et al. [13] presented

a method to model anechoic boundaries. The mesh topology used has a significant impact on the dispersion error in the model. This is the error in the direction and magnitude of the sound propagation. The most common meshes are rectilinear and triangular. Detailed comparison of mesh topology were presented by Murphy et al. [14] and Campos et al. [15].

This paper is organised as follows. The theory section gives an overview of the image source method. Two case studies are then presented. Both deal with areas of live musical performance and investigate whether the room absorption can be optimised to improve certain aspects of the mix. The first seeks to maximise the vocal level in the monitor mix, relative to other instruments on stage. The second attempts to reduce the effect of acoustic feedback, which often restricts the amount of gain that can be applied to microphone input signals. A discussion of the results follows.

## 2. THEORY

The image source method is used to model the acoustic signal path from source to listener. The limitations of this model are detailed in Section 1. The two main limitations are; the minimum frequency below which room effects become significant, and the treatment of reflections as being specular. Whilst these are significant assumptions when modeling a complete room response, the work here is focussed on the re-enforcement effects of early reflections only, which will be subject to less diffusion effects. The analysis here is also being performed independent of signal frequency. It is understood that frequency will affect wall absorbency, reflection angles, microphone response and many other phenomena. As this is an initial study into the potential optimisation of enclosure absorption these effects have been omitted. The acoustic path from source to listener is modeled as an acoustic gain.

The image source model places image sources to represent the room reflections as shown in Figure 1. The shaded rectangle is the original room. Sources (both real and image) are identified by an  $X$ , the receiver is identified by a  $+$ , and the reflection points are identified by an  $O$ . For clarity, not all reflection paths have been plotted. The signal experienced at

the listener location is a combination of all image paths. The intensity of the signal in each signal path decreases with distance following the inverse square law, assuming each source is a unit sphere of radius  $1m$ . Each time the path crosses a boundary an attenuation is applied based on the respective absorption coefficient,  $\alpha$ . It is assumed that the reflection coefficient is independent of frequency and angle of incidence. The sound pressure level (SPL) of the signal is multiplied by a scalar, where a value of 1 represents a fully reflective boundary and a value of 0 reflects a fully absorbent boundary.

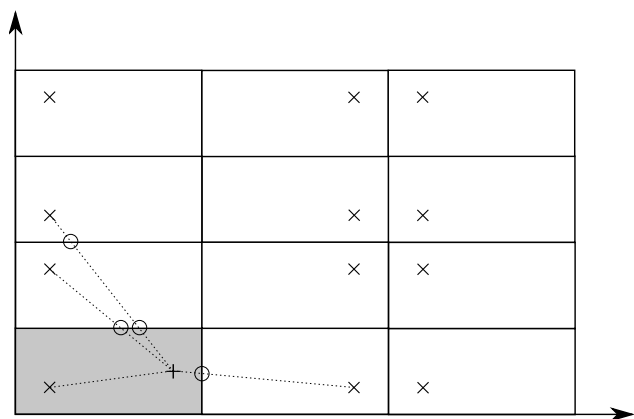


**Fig. 1:** Illustration of the image source model, x - source, + - listener, o - reflection point

Aspects of live musical performance are to be investigated. The perception of a source is subject to psychoacoustic effects. The Haas effect dictates that any sounds which occur within  $20\text{-}30ms$  will be experienced as a single acoustic event [16]. This is an important effect when considering live musical performance, particularly in a small enclosure. The proximity of reflections reaching a listener relative to the direct sound means that the reflections will have a re-enforcing effect on the direct sound, making the original source sound louder. This is an intuitive result. Sounds made within a small enclosure will sound louder. The effect is not so significant for large rooms as fewer (if any) reflections will reach the listener within the Haas time. In large rooms early reflections may be heard as distinct echoes, but it is also likely that they will form the diffuse reverberant field.

The Haas time is used to identify the set of reflections which have a re-enforcement effect on the direct sound. The upper limit on the Haas time is used, which is  $30ms$ . All reflections which reach the listener within  $30ms$  of the direct sound are combined to calculate the perceived SPL of the signal. It is acknowledged by the author, that alternative loudness measures which are frequency dependent are more appropriate in determining the perceived level. The work here is performed independent of frequency so this does not apply. If  $A_{Dij}$  is the direct acoustic path from source  $j$  to listener  $i$ , and  $A_{Rnij}$  is reflected acoustic path  $n$ , then the total perceived acoustic path  $A_{Tij}$  from source to listener is,

$$A_{Tij} = 20\log_{10} \left[ 10^{\frac{A_{Dij}}{20}} + \sum_{n=1}^N \left( 10^{\frac{A_{Rijn}}{20}} \right) \right], \quad (1)$$

where  $N$  is the total number of reflections which reach the listener within  $30ms$  of the direct sound.

### 3. CASE STUDIES

The case studies examined are based around a typical small room. Analysis is performed in two dimensions. Inclusion of the third dimension would increase the re-enforcement effect, assuming that the reflections in this dimension reach the listener within the Haas time. The model is restricted to two dimensions for simplicity in this early study. The dimensions of the room are  $8m \times 15m$ . Each wall is divided into  $1m$  sections. The absorption coefficient of each section of the wall is defined independently, and can have a value from 0 (fully absorbent) to 1 (fully reflective). Once the case study has been defined the absorption parameters for each part of the room are optimised to best satisfy the objectives. In both case studies it is assumed that the sources have the polar dispersion pattern shown in Figure 2.

#### 3.1. Monitor Mix

The first element of a live performance to be examined is the monitor mix. At small venues there is often great difficulty in getting the vocal level sufficiently high in the mix. Whilst the entire monitor mix is not considered here, a simplified example which is representative of the problems involved is

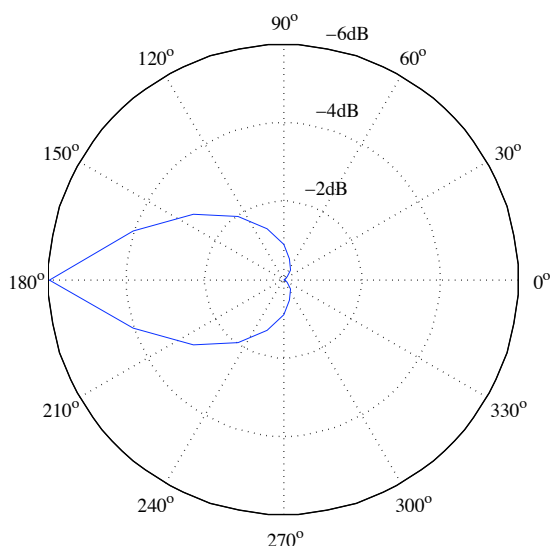


Fig. 2: Polar dispersion profile of all sources

presented. Figure 3 a) shows a typical stage setup in the small room detailed above. The area from 0 to 5m on the x axis represents the stage. The setup consists of a vocalist, guitarist, bassist, drummer and 3 monitor speakers (left, center and right), indexed from one to seven respectively. Sources one to four are aligned at 0° to the x axis. Sources five to seven are aligned at 200°, 180° and 160° to the x axis respectively. It is assumed that the vocal only is going through the monitor speakers, and that the gain that has been applied is at the maximum possible before the onset of acoustic feedback. The goal is to adjust the wall absorbcency parameters to maximise the acoustic signal path from the monitor speakers to the vocalist, whilst minimising the acoustic paths from the other instruments to the vocalist. In this way the vocal level in the monitor mix will be increased. It is worth noting that changing the wall absorption parameters will change the potential onset of feedback. This effect is omitted here.

The error function to be minimised is given in Equation 2. It is the inverse of the combined magnitude of all monitor speaker paths, minus the combined magnitude of all other source paths. The vocal source (source 1) has been omitted from this equation. Although the vocals will contribute to the overall vocal

level, it is assumed here that the acoustic level of the vocals is insignificant when compared to the amplified level coming out of the monitor speakers.

$$e = \frac{1}{20 \log_{10} \sum_{n=5}^7 10^{\frac{A_{Tijn}}{20}} - 20 \log_{10} \sum_{m=2}^4 10^{\frac{A_{Tijm}}{20}}} \quad (2)$$

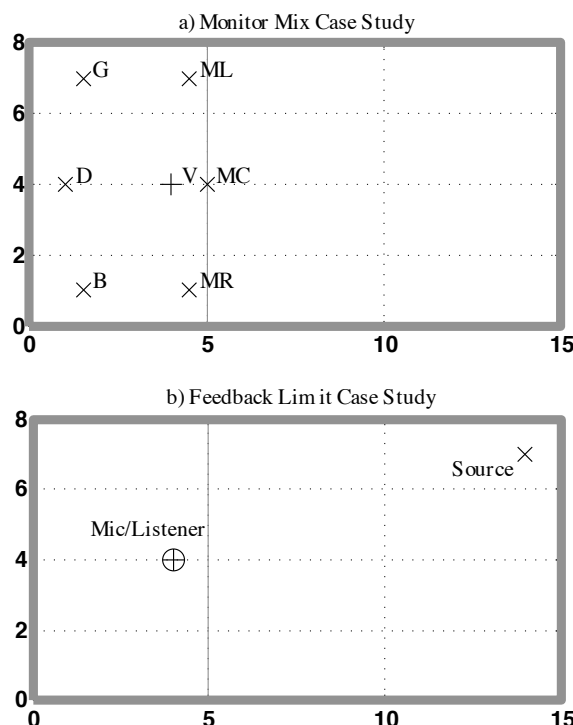


Fig. 3: Small venue case study setup, a) Monitor mix case study, M - monitor speaker (left, center and right), V - vocalist, G - guitar amplifier, B - bass amplifier, D - drum kit, b) Feedback limit case study.

The optimal wall parameters are found using the Matlab *fmincon* function, which minimises the error function (Equation 2) subject to side constraints. The side constraints limit the wall absorbcency parameters between 0 and 1. The algorithm uses a steepest descent, gradient method. Table 1 shows the acoustic signal path gain of the six sources for four different absorbcency configurations; anechoic where  $\alpha = 0$ , partially reflective where  $\alpha = 0.5$ , fully reflective where  $\alpha = 1$  and optimised, where

the absorption coefficient for each wall element has been optimised. It also shows the combined signal path of all instruments and monitors, and the vocal headroom, which reflects the level by which the combined monitor acoustic path gain exceeds the combined acoustic path gain of the other instruments. It can be seen that the case where the room absorption has been optimised has a significantly greater vocal headroom.

**Table 1:** Monitor Mix Case Study Results

Source	$\alpha = 0$	$\alpha = 0.5$	$\alpha = 1$	$\alpha = \alpha_{opt}$
Guitar	-12.1	-6.1	-2.6	-12.1
Bass	-12.1	-6.1	-2.6	-12.1
Drums	-9.5	-5.4	-2.6	-9.5
Mon L	-10.1	-5.4	-2.3	-2.9
Mon C	0.0	1.4	2.5	1.8
Mon R	-10.1	-5.4	-2.3	-2.9
Inst Gain	-1.6	3.7	7.0	-1.6
Mon Gain	4.2	7.0	9.2	8.5
V Headroom	5.8	3.3	2.2	10.1

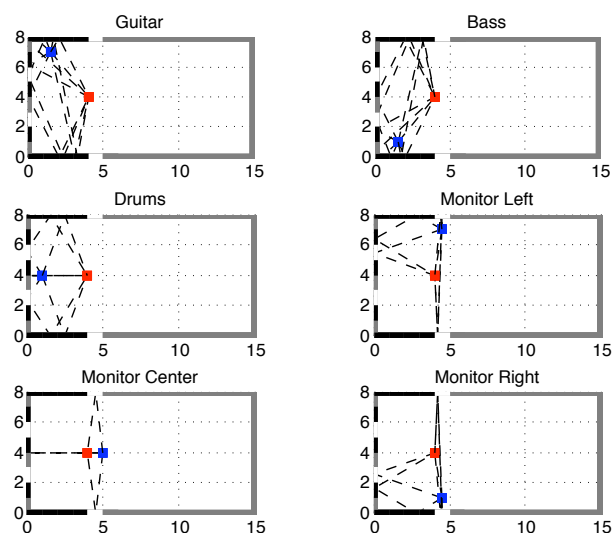


**Fig. 4:** Reflection paths from each source to the vocalist location, which occur within the Haas time

Figure 4 shows the reflections which have been in-

cluded in determining the total SPL at the listener location. The color of each wall segment identifies the absorption coefficient. If the wall segment is white it is fully reflective and if it is black it is fully absorbent. There is a linear scale in between. It can be seen that for this monitor mix case study only reflections within the stage area reach the listener within the Haas time. The areas immediately adjacent to the the monitor speakers are fully reflective, which will increase their effective power. The opposite is true for the other instruments, which are situated near to wall segments of high absorbency.

### 3.2. Feedback Limits

The second element of a live performance to be examined is the onset of acoustic feedback. Acoustic feedback is a static phenomena and will occur if the loop gain of a microphone and speaker combination is greater than  $0dB$  and is frequency dependent. During a performance, a buffer of around  $3dB$  is used to prevent the sudden onset of feedback due to unexpected amplification or room acoustic events. Feedback becomes an issue when the maximum loop gain prevents further amplification, but the level is too low in either the front of house or monitor mix. This is often experienced with vocals, but can occur with any source that has a low signal compared to other instruments on stage, for example a violin which is positioned close to the drum kit on stage. The objective of this study is to optimise the room absorption parameters to maximise the acoustic path gain from speaker to listener, whilst minimising the feedback loop gain. The example setup used is shown in Figure 3 b). The source is aligned at  $270^\circ$  to the x axis. The room absorption optimisation is performed for a range of microphone alignment, from  $0^\circ$  to  $360^\circ$ . The feedback is treated as being independent of frequency. It is assumed that the listener is positioned at the same location as the microphone. The listener is omnidirectional, but the microphone has a cardioid polar response pattern. This pattern is shown in Figure 5 and is representative of a Shure SM58 at  $1KHz$ . It is also assumed that the Haas effect applies to the input of the microphone.

The error function to be minimised is given in Equation 3. Minimisation of this function will give the distribution of absorbency around the room which

maximises the vocal level heard relative to the microphone input. This effectively raises the vocal level heard before the onset of acoustic feedback, and the difference between these two gain values is defined as the feedback headroom.

$$e = \frac{1}{A_{T\text{listener}} - A_{T\text{microphone}}}. \quad (3)$$

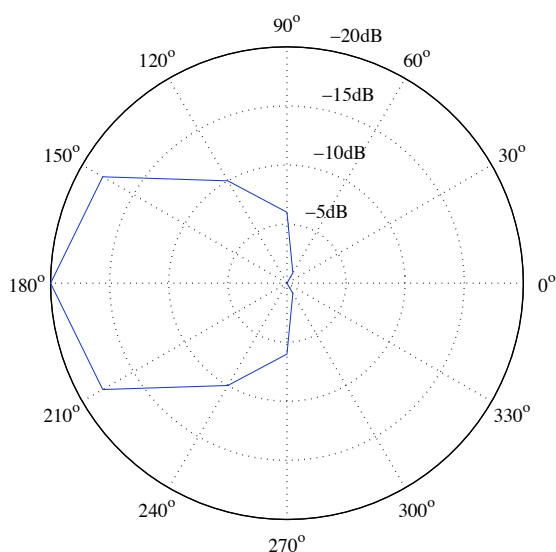


**Fig. 5:** Polar response pattern of microphone, modeled on Shure SM58 at 1KHz.

Table 2 contains the feedback headroom for a number of microphone orientations and room absorption configurations. The absorption parameters in the optimal configuration have been evaluated independently of the monitor mix case study. In all absorption configurations the headroom is reduced when the microphone is facing the speaker (microphone angle = 0°). This is the expected result. Any musician will attest that pointing the microphone at a speaker is a bad idea! The difference in feedback headroom over the angles investigated is more significant when the walls are highly absorbent. This is because reflective surfaces cause the sound to approach the listener from a range of directions, limiting the effect of the microphone polar pattern. The optimised absorption configuration shows the best feedback headroom for all microphone orientations.

**Table 2:** The feedback headroom for a range of microphone orientations and room absorption configurations.

Mic Angle	$\alpha = 0$	$\alpha = 0.5$	$\alpha = 1$	$\alpha = \alpha_{opt}$
0°	0	1.7	2.0	4.5
90°	8.2	5.9	5.5	8.7
180°	18.9	10.6	9.6	18.9
270°	3.2	4.6	4.9	7.3

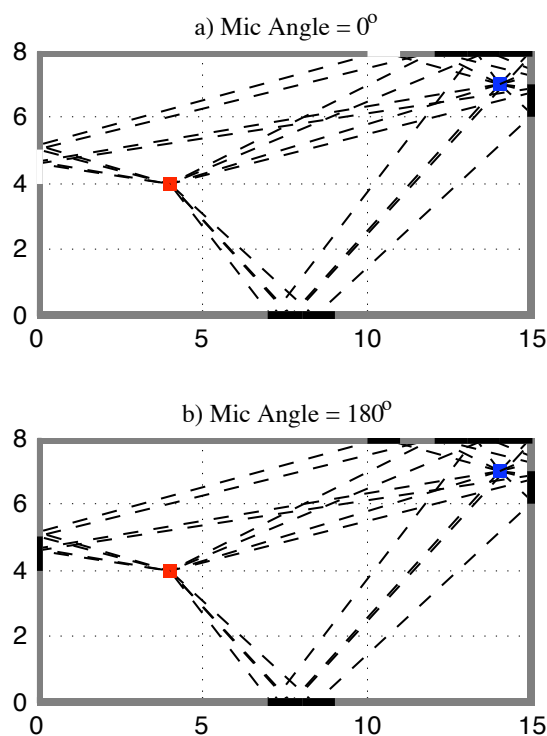


**Fig. 6:** Reflection path from source to listener / microphone in feedback case study, a) microphone angle = 0°, b) microphone angle = 180°.

Figure 6 a) and b) show the reflection paths and optimised absorptency for microphone angles of  $0^\circ$  and  $180^\circ$  respectively. The key differences in the distributions are at coordinates (0, 5) and (8, 10). When the microphone is facing the loudspeaker, the headroom is maximised by ensuring maximum reflection strength from the wall behind the microphone. When the microphone is facing away from the loudspeaker, the headroom is maximised by ensuring minimum reflection strength.

#### 4. DISCUSSION

Two case studies have been presented. Both deal with areas of live musical performance and investigate whether the room absorption can be optimised to improve certain aspects of the mix. The author accepts that some of the assumptions made in using the image source model are crude, and that they would put a severe limit on the accuracy of a predicted room response. The results however do highlight optimal absorption configurations which are intuitively correct, and are used in practice. Putting sources near to reflective walls will increase their effective power, and making the back wall on stage highly absorbent will reduce the tendency for feedback. Modeling these phenomena individually seems like overkill if the outcome is already known. However, if these elements are combined with a more comprehensive model of a live performance, for example including monitor mixes for each performer and the front of house mix, automatic optimisation becomes more useful. This could not only include room absorption coefficients, but also stage setup and mixer settings.

A key assumption made in this work was the use of the Haas time to identify early reflections which have a re-enforcement effect on the direct sound. In making this assumption it is being assumed that the listener has no interest in the reverberant field after this time. From the authors' personal experience, this is a valid assumption, particularly when considering the monitor mix. The most important factor is the relative volume of each instrument. The effect of the reverberant field will however, become more significant as the size of the venue increases. The use of the Haas time to model the onset of acoustic feedback is a more contentious assumption. It is clearly necessary to include reflections in the feedback loop gain, but the cutoff time is less obvious.

Feedback is a frequency dependent phenomenon so it will depend to an extent on the phase of the signals reaching the microphone. For real signals however, particularly after reflections, it is unlikely that signals will be coherent, so looking at phase relationships is less meaningful. It is the intention of the author to examine feedback phenomena experimentally to ascertain an equivalent Haas time for the onset of acoustic feedback.

#### 5. CONCLUSION

A method has been presented which optimises the distribution of absorption around an enclosure. Two case studies are used to illustrate the method. The monitor mix case study seeks to maximise the vocal level relative to the combined level of all other instruments. The feedback case study seeks to maximise the feedback headroom. In both cases the optimised absorption is an improvement on anechoic, partially reflective and fully reflective rooms. It has been assumed that the Haas time for the human perception of sound signals is applicable to acoustic feedback. This is a significant assumption. A study into the effective Haas time for microphones for the onset of acoustic feedback is a further interesting area of study that would be required to verify this work. Whilst the limitations of the model prevent accurate room response predictions, the results are intuitively correct, and pave the way for more advanced live performance problems and models to be studied.

#### 6. REFERENCES

- [1] Heinrich. Kuttruff. *Room acoustics / Heinrich Kuttruff*. Applied Science Publishers, London :, 2d ed. edition, 1979.
- [2] A. Krokstad, S. Strom, and S. Sorsdal. Calculating the acoustical room response by the use of a ray tracing technique. *Journal of Sound and Vibration*, 8(1):118–125, July 1968.
- [3] D. K. Jones B. M. Gibbs. A simple image source method for calculating the distribution of sound pressure levels within an enclosure. *Acustica*, 26:24–32, 1972.
- [4] D. A. Berkley J. B. Allen. Image method for efficiently simulating small-room acoustics. *The Journal of the Acoustical Society of America*, 65(4), 1979.

- 
- [5] Murray Hodgson. Evidence of diffuse surface reflection in rooms. *The Journal of the Acoustical Society of America*, 88(S1):S185–S185, 1990.
- [6] B. I. L. Dalenback. Room acoustic prediction based on a unified treatment of diffuse and specular reflection. *Journal of the Acoustical Society of America*, 100(2):899–909, 1996.
- [7] J. J. Embrechts. Broad spectrum diffusion model for room acoustics ray-tracing algorithms. *The Journal of the Acoustical Society of America*, 107(4):2068–2081, 2000.
- [8] Bengt-Inge Dalenback, Peter Svensson, and Mendel Kleiner. Room acoustic prediction and auralization based on an extended image source model. *The Journal of the Acoustical Society of America*, 92(4):2346–2346, 1992.
- [9] J. BORISH. Extension of the image model to arbitrary polyhedra. *The Journal of the Acoustical Society of America*, 75(6):1827–1836, 1984.
- [10] D. Murphy, A. Kelloniemi, J. Mullen, and S. Shelley. Acoustic modeling using the digital waveguide mesh. *Signal Processing Magazine, IEEE*, 24(2):55–66, 2007.
- [11] L. Savioja, T. J. Rinne, and T. Takala. Simulation of room acoustics with a 3-D finite difference mesh. In *Proc. Int. Computer Music Conf.*, pages 463–466, Aarhus, Denmark, September 194.
- [12] Kyogu Lee and Julius O. Smith. Implementation of a highly diffusing 2-d digital waveguide mesh with a quadratic residue diffuser. In *Proc. of the Int. Computer Music Conf*, 2004.
- [13] D. T. Murphy and J. Mullen. Digital waveguide mesh modelling of room acoustics: Improved anechoic boundaries. In *Proc. Intl. Conf. Digital Audio Effects (DAFX-02)*, pages 163–168, Hamburg, Germany, September 2002.
- [14] D.T. Murphy and D.M. Howard. Digital waveguide modelling of room acoustics: Comparing mesh topologies. *EUROMICRO Conference*, 2:2082, 1999.
- [15] G.R. Campos and D.M. Howard. On the computational efficiency of different waveguide mesh topologies for room acoustic simulation. *Speech and Audio Processing, IEEE Transactions on*, 13(5):1063–1072, Sept. 2005.
- [16] D.M. Howard and J. Angus. Acoustics and psychoacoustics. *Focal Press*, 2006.